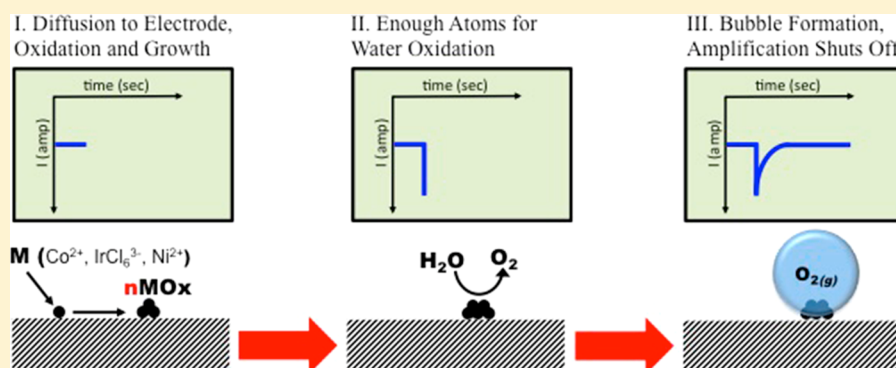


Toward the Digital Electrochemical Recognition of Cobalt, Iridium, Nickel, and Iron Ion Collisions by Catalytic Amplification

Jeffrey E. Dick and Allen J. Bard*

Center for Electrochemistry, Department of Chemistry, The University of Texas at Austin, Austin, Texas 78712, United States



ABSTRACT: We report the electrochemical detection of femtomolar amounts of cobalt, iridium, nickel, and iron ions in solution by electrocatalyst formation and amplification. The metal oxides of these ions can be formed electrochemically and can catalyze the oxidation of water. Alternatively, the reduction of metal ions to metals, such as the reduction of IrCl_6^{3-} to iridium, is capable of electrocatalytically reducing protons to molecular hydrogen, as shown previously with Pt. These events, which manifest themselves in amperometry, correspond to the formation of electrocatalytic nuclei on the electrode surface, capable of electrocatalytically oxidizing water or reducing protons. An analysis of the frequency of anodic blips compared to theory implies that the requirement for water oxidation is 10 ± 1 ions of cobalt, 13 ± 4 ions of iridium, and 11 ± 3 ions of nickel. A similar analysis for iridium reduction and the corresponding catalytic reduction of protons implies that 6 ± 2 ions of iridium are required for proton reduction. These numbers are confirmed in an analysis of the time of first nucleation event, i.e. the time at which the first blip on the amperometric $i-t$ experiment occurs. We further show that the anodic blips in detecting nickel increase in intensity upon increasing amounts of iron ions in solution to a ratio of Ni/Fe of ~ 5 , surprisingly close to that for bulk electrocatalysts of Ni-Fe.

INTRODUCTION

The study of electrocatalytic reactions, such as the oxygen evolution reaction (OER) or the hydrogen evolution reaction (HER), has been extensively pursued over the past century. Fundamental studies into the mechanism of water oxidation and proton reduction on these various heterogeneous electrocatalysts have been carried out on bulk materials composed of “ensembles” of a huge number of atoms (even for nanostructures) by electrochemical techniques such as voltammetry. Calculations by density functional theory, usually based on the energetics of surface species, claim to validate mechanisms and relative rates. Questions about how these electrocatalysts form and the minimum number of atoms necessary to catalyze a reaction are as yet unanswered as are those dealing with nanoparticle size and morphology effects on catalysis.

Recently, we reported the observation of amperometric blips corresponding to the discrete nucleation of electrocatalytic clusters of platinum ($n = 5 \pm 1$ atoms) from solutions containing femtomolar amounts of PtCl_6^{2-} ion.¹ Briefly, the carbon fiber ultramicroelectrode (UME) was held at a potential in a 1 M H_2SO_4 solution where proton reduction will occur on

platinum but not on carbon. Discrete blips can be observed upon addition of femtomolar amounts of platinate salt, which will reduce to platinum atoms at the applied potential. From an analysis of frequency of events, we estimated that 5 ± 1 atoms of platinum were on the surface of the electrode when a blip was observed. This observation implies that about 5 atoms of platinum are required to induce proton reduction, and the results match well with other studies on effects of cluster size on electrocatalytic activity.^{2,3} The observation of a blip-like response can be explained by the formation of a bubble of hydrogen gas on the catalytic cluster, which shuts off further catalysis. The formation of nanobubbles and the electrochemical response of generating a nanobubble on a platinum nanoelectrode have been well characterized.⁴ Because of the formation of a nanobubble, the continuous observation of the growth of a cluster cannot yet be studied. A similar schematic can be imagined for the production of electrocatalytic clusters of water oxidation catalysts, such as cobalt oxide, iridium oxide,

Received: March 28, 2016

Published: June 13, 2016

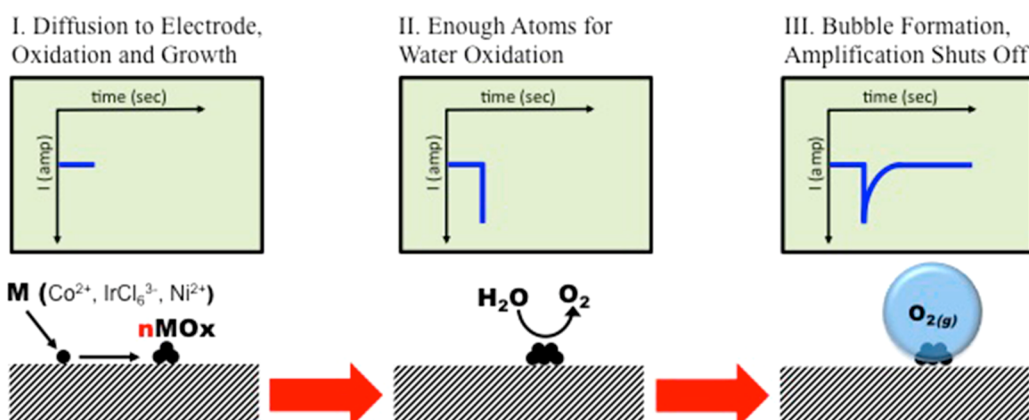


Figure 1. Schematic representation of the OER experiment. In Step I, diffusion is the main source of mass transfer of ions to the surface of the electrode. In Step II, oxidized ions will form on the surface to create a critical nucleus size, capable of catalysis. In Step III, this catalysis is shut off due to the formation of an O_2 bubble at the cluster.

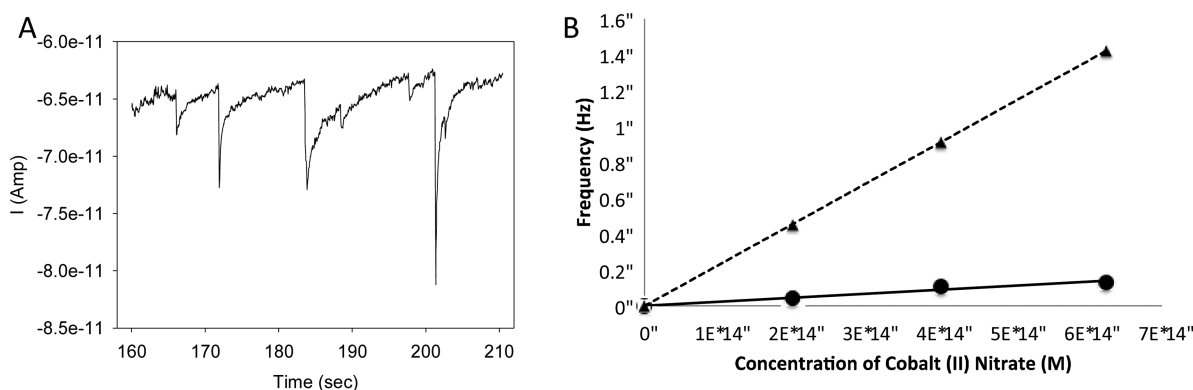


Figure 2. (A) Representative $i-t$ response of 62.5 fM cobalt nitrate solution on a 10 μm carbon fiber UME. Experiments were carried out with 10 mM phosphate buffer, pH = 7.4. Experiments were performed at room temperature in air. The amperometric sampling rate was 50 ms. (B) Frequency versus concentration curves for experimental results (solid line) compared to theoretically calculated collision frequencies of the cobalt ions (dashed line).

nickel oxide, and nickel–iron oxide from femtomolar solutions of the ionic precursors under neutral pH conditions.

Figure 1 gives a schematic representation of the experiment. Ions diffuse from the bulk solution and are oxidized at the surface of the electrode. We assume they diffuse on the surface, nucleate at a given site, and grow on the electrode.⁵ The oxidation of single ions involves a few electrons, which cannot be detected against the background. Thus, a catalytic reaction is necessary to observe a response. When enough oxidized atoms nucleate into an active cluster, the electrocatalytic reaction (OER) can be driven at these small clusters, producing the amperometric blip. An O_2 bubble forming on the catalyst surface, effectively shutting off the reaction, likely causes the deactivation of each cluster. In our model, the bubble isolates the cluster and shuts off the catalysis. Furthermore, we cannot rule out other reactions, such as the oxidation of the carbon electrode, which could also contribute to the Faradaic response. The nature of the substrate and impurities in solution may affect the calculated cluster size with our method. The electrode potential on the carbon fiber UME was biased between 1 and 1.4 V versus Ag/AgCl for these experiments. At these potentials, the ions will be oxidized upon interaction with the electrode surface. Also at these potentials, the electrocatalytic oxidation of water can occur on the metal oxide catalysts, but not on the carbon electrode.

EXPERIMENTAL SECTION

Chemicals. Water used in each experiment was Milli-Q water (Massachusetts, USA). Cobalt(II) nitrate, $K_3\text{IrCl}_6$, nickel(II) nitrate, and ferrous chloride were purchased from either Sigma Aldrich or Fisher Scientific and used without further purification. Phosphate buffer saline was purchased from Fisher Scientific as a stock solution and diluted for the experiments. Nanopure water was used throughout each experiment to ensure low levels of ionic contaminants and dissolved organic matter.

Electrochemistry. Electrochemical experiments were carried out using a CHI model 900B potentiostat (CH Instruments, Austin, TX). The three-electrode cell was placed in a Faraday cage, which was grounded to a water pipe. The sampling rate for each amperometric $i-t$ experiment was 50 ms unless otherwise noted. A commercial reference electrode (Ag/AgCl, BASi, West Lafayette, IN) was employed in the cell, and a platinum wire, graphite rod, or tungsten rod was employed as the auxiliary electrodes. Generally, experiments were performed in a 20 mL glass vial with a cap to position the electrodes in the solution.

Preparation of UMEs. The carbon fiber UME was prepared following a general procedure.⁶ Briefly, UMEs were prepared by sealing a 10 μm diameter carbon fiber in a borosilicate capillary using resistive heating. Silver epoxy was used to establish a connection to a nickel–chromium wire. The electrode was then polished to expose the active surface of the carbon. After each experiment, electrodes were mechanically polished using wetted diamond polishing pads and treated with a nitric acid bath.

Preparation of fM solutions. Preparation of fM solutions of accurate concentration is difficult because of nonspecific adsorption and errors during dilution, such as propagation of error while pipetting. Four initial volumetric flasks were prepared with 1 mM of the analyte of interest. These flasks were allowed to sit at room temperature in a dark environment for 48 h. After 48 h, flasks were poured out, and another 1 mM solution of the analyte of interest was placed in the flask and allowed to equilibrate for 48 h. This process occurred a total of 3 times before the flasks were emptied and the solutions were made for the electrochemical analysis. After these initial solutions, we equilibrated flasks with more dilute solutions 5–10 times each until the desired concentration was reached. For the final solutions, serial dilutions were made by pipetting 10 μL of the initial solution into 10 mL of the solvent inside an equilibrated flask until concentrations of picomolar were achieved. Four flasks were necessary because the beginning solution generally had mM amounts of analyte (mM to μM to nM to pM). From this stock solution of picomolar amounts of analyte, samples were taken for the electrochemical analysis, which were completed in vials that were equilibrated as previously discussed. Each volumetric flask was initially calibrated by a 5 mL micropipette.

RESULTS AND DISCUSSION

Femtomolar Detection of Cobalt. Ions of cobalt were detected by holding the potential of the electrode such that the

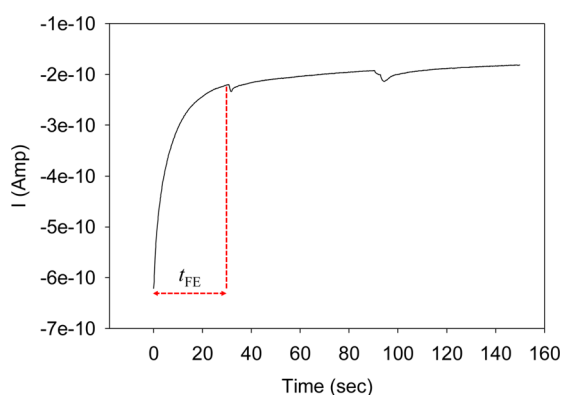


Figure 3. Time of first event example for experiments with 15 fM cobalt nitrate. Experiments were carried out under neutral pH conditions with phosphate buffer, pH = 7.4. Experiments were performed at room temperature in air. The amperometric sampling rate was 50 ms.

metal oxide will electrodeposit and water oxidation can be catalyzed on the metal oxide but will not readily occur on the relatively inert carbon fiber UME. The potentials chosen were between 1.2 and 1.4 V vs Ag/AgCl given that the deposition potential for bulk Co^{2+} is around 1.0 V vs Ag/AgCl.⁷ Upon addition of femtomolar amounts of ions, anodic current spikes were observed in the amperometric $i-t$ response.

Figure 2A gives examples of the common spikes observed in each experiment for cobalt. Generally, the spikes would occur and then exponentially decay to the background steady-state current. We attribute this decay to the formation of a bubble of oxygen gas at the nucleation site. According to White and co-workers, who studied bubble formation on nanoelectrodes, bubble formation rapidly cuts off any electrocatalytic reaction being carried out at the electrode; however, the reaction is still driven on a small (<1 nm) ring about the electrode that is not covered by the bubble. The decay is slower when we compare the decay of the OER catalytic clusters to the previously reported decay of the HER on small platinum nuclei from

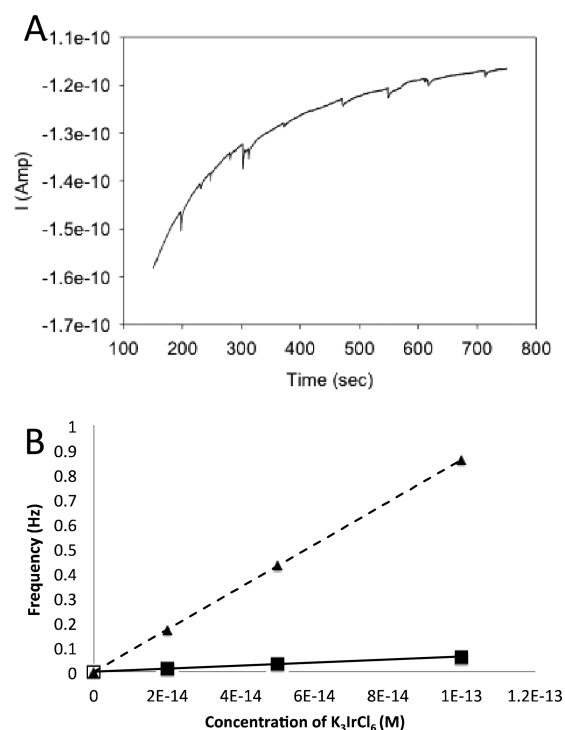


Figure 4. (A) Representative $i-t$ curve for experiments with femtomolar concentrations of iridium. (B) Frequency versus concentration curves for various concentrations of iridium salt. The solid line represents the experimental results, and the dotted line represents the calculated values. Experiments were carried out under neutral pH conditions with phosphate buffer, pH = 7.4. The amperometric sampling rate was 50 ms.

femtomolar platinate solutions. The difference in this decay rate could be due to the higher solubility of oxygen in neutral pH water than hydrogen gas in 1 M H_2SO_4 solutions. Figure 2A displays event examples with 62 fM cobalt(II) nitrate in solution.

The diffusive flux of the ions to the electroactive surface can be understood in a stochastic sense by using the frequency, f , with which an ion collides with the electrode under diffusion control, given by

$$f = 4DCrN_A \quad (1)$$

where D is the diffusion coefficient of the ion, C is the concentration of the ion, r is the radius of the inert substrate electrode, and N_A is Avogadro's Number. Thus, the theoretical frequency with which ions collide with the electrode can be calculated by easily known values, i.e. diffusion coefficients in water, the concentration, and the radius of the UME. The results can then be compared to the frequency of blip formation in the presence of a certain concentration of ions. From this information, an average number of ions that have collided with the electrode surface before the OER occurs can be obtained. One key assumption in these calculations is that the adatom (or adatom oxide) is able to freely diffuse on the electrode surface upon oxidation until it is immobilized at a suitable surface nucleation site, and other adatom oxides find the growing nucleus.⁸

Figure 2B shows the frequency versus concentration data for experiments with varying concentrations of cobalt nitrate in solution (solid line). It should be emphasized that the observed events are catalytic clusters capable of water oxidation. The

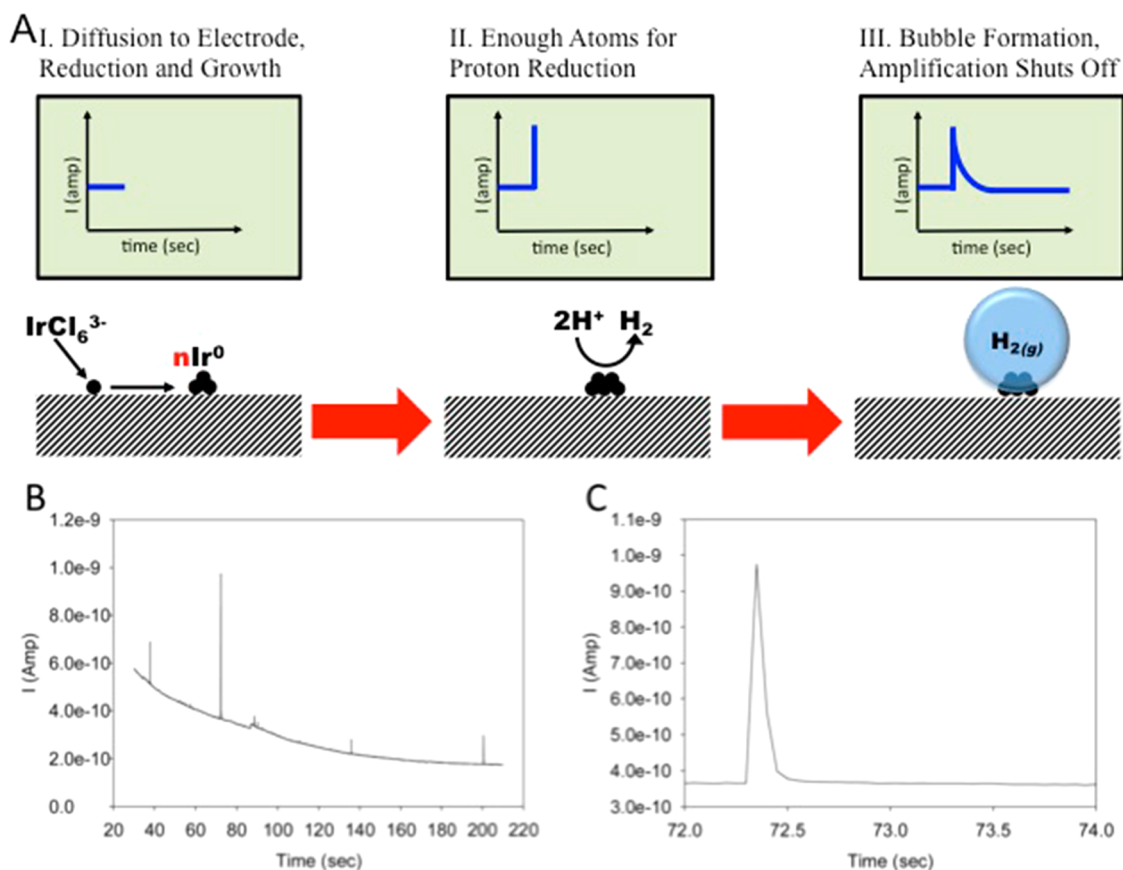


Figure 5. (A) Schematic representation of the proton reduction experiment with hexachloroiridium. (B) Amperometric $i-t$ experiment with 20 fM hexachloroiridium in 1 M H_2SO_4 under ambient conditions. The sampling rate was 50 ms. (C) Enlargement of blip response.

dotted line is the calculated frequency versus concentration curve for freely diffusing ions. By comparing these two different curves, one can deduce the average number of cobalt ions that have interacted with the electrode surface before an event is observed. For cobalt nitrate, this value was ~ 10 ions. There are several assumptions that go into this model, which invokes classical nucleation and growth theory on UMEs.⁹ In classical nucleation and growth theory, it has been shown that a single center can form on electrodes of micrometer dimensions. When a nucleus is formed, it forms an exhaustion zone that limits the possibility of nucleation around the nucleation site. On carbon, it may also be a function of the extent of coverage of impurities on the surface of the electrode. There are also other assumptions. For instance, we assume that ions are oxidized with a unit efficiency and stick to the electrode surface. These ions are then able to freely diffuse until they find a low-energy well or surface defect. In classical nucleation and growth theory, UMEs have been used as a means of growing a single center. The cluster formation is governed by the low concentration of ion, which means that the diffusion of ions to the electrode surface is the rate-determining step if 2D diffusion on the surface of the electrode is fast. We also assume that the concentrations of ions are approximately correct, which is demonstrated by the linearity in the frequency versus concentration curve and the intersection of each curve very near the origin.

A similar electrochemical measurement of the number of ions that have interacted with the surface of the electrode can be obtained by considering the time of first event (t_{FE}), which is displayed in Figure 3. The average time is simply the inverse of

the frequency of collision. This time of first event can be calculated using the inverse of eq 1 assuming the flux of the ions to the electrode surface is governed by diffusion only. In these experiments, the electrode was switched on immediately after being submerged in the solution of cobalt ions. When ions were present, the time of the first anodic event was recorded. In Figure 3, the time of first event is 32 s, and the concentration was held at 15 fM, implying that about 11 ions of cobalt were required to cause an event. Throughout experiments, similar numbers (11 ± 2 ions of cobalt) of ions using the time of first event were found compared to the frequency analysis. This implies that the flux of ions to the electrode surface is diffusion controlled and matches the prediction from the inverse of eq 5.

Femtomolar Detection of Iridium. Ions of iridium were also observed by nucleating catalytic clusters that had the ability to oxidize water in accord with Figure 1. Figure 4A displays the common collision events observed with iridium in solution for the water oxidation mechanism. From our previous work with iridium oxide nanoparticles,¹⁰ the potential was chosen such that water oxidation would occur on iridium but not on the carbon fiber UME (0.8 V vs Ag/AgCl). Therefore, each discrete event corresponds to the nucleation of a catalytic cluster of iridium oxide moieties on the electrode surface. Figure 4B gives the frequency versus concentration curve for experiments with different concentrations of iridium.

A similar analysis of frequency versus concentration as carried out for cobalt can be applied to the iridium experiments. From this, we find that 13 ± 4 ions of iridium are required to display an event. Experiments using t_{FE} as the measured value

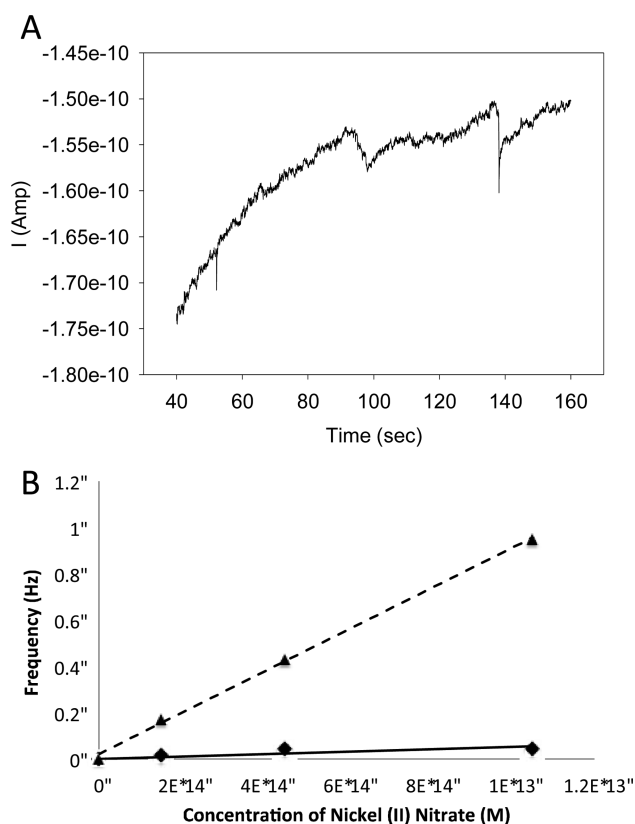


Figure 6. (A) Amperometric experiment with nickel nitrate in femtomolar concentrations. The sampling rate was 50 ms, and the applied potential was 1.4 V vs Ag/AgCl. (B) Frequency versus concentration for nickel(II) nitrate (solid line) compared to theoretical prediction based on diffusion (dotted line).

displayed similar values (10 ± 3 ions) to those of the frequency analysis

Alternatively, another mechanism for femtomolar detection of iridium ions can be envisioned based on previous work.¹ Iridium metal catalyzes the reduction of protons in acidic media compared to an inert carbon surface. Figure 5A gives a schematic representation of the experiment, which is similar to the schematic in Figure 1 except instead of catalyzing water oxidation, the deposited catalytic cluster will catalyze proton reduction. In this experiment, the potential is held such that the iridium ions will be reduced to an iridium metal at the electrode surface. The removal of oxygen is critical in these experiments for reproducibility; therefore, each solution was bubbled with argon gas for at least 15 min, and an argon gas blanket was placed over the solution during the experiment. When a catalytic cluster is formed that is stable enough to catalyze proton reduction, an electrocatalytic amplification of current is expected. Figure 5B shows the general $i-t$ response for 20 fM iridium ions in solution on an inert carbon fiber UME biased at -0.5 V vs Ag/AgCl. The solution was degassed for 15 min with argon to rule out any oxygen reduction effects on the cluster growth mechanism. Interestingly, it was found that 6 ± 2 ions of iridium were required to catalyze proton reduction using the frequency analysis employed before, which is about half the number of ions required for water oxidation, but essentially the same as the Pt metal cluster for the HER.

Femtomolar Detection of Nickel and Increased OER Activity with Iron. The electrocatalytic amplification of small clusters is also feasible in detecting nickel ions in solution,

which oxidize to form a nickel oxide that will catalyze water oxidation against the carbon fiber UME background. Figure 6A shows the usual $i-t$ response in the presence of nickel nitrate in femtomolar concentrations, and Figure 6B gives the frequency versus concentration curve.

The search for electrocatalysts for the OER has extended to combining low-cost, earth abundant metals to obtain higher reactivity. The introduction of iron into the nickel solution has been shown to enhance the OER rate upon deposition.^{11,12} Iron oxide is a poor catalyst; however, in the presence of nickel, the catalysis of the OER is enhanced. Berlinguette and co-workers showed that when nickel and iron were in a 5:1 ratio, the mixture displayed the best catalytic activity toward water oxidation by screening several mixtures of nickel, and iron, oxides. The exact mechanism of the nucleation and growth from the very initial stages of nucleation has not been well studied, and we were interested if this effect could be seen using stochastic electrochemistry.

Surprisingly, upon introduction of iron ions (from ferrous chloride) into a solution of 100 fM nickel ions, current peak heights increased to a maximum of about 40 pA and then decreased. Figure 7A shows the usual current–time transients for the experiments with increasing amounts of iron ions in solution, and Figure 7B–C are enlargements of some of the representative peaks observed. By comparing Figure 7A to Figure 6A and the background given in Figure 7A (black trace), there is an increase in blip height in the presence of ferrous chloride. From the figure the height of the events increased with increasing amounts of iron when compared to Figure 6A with only nickel ions. Figure 7B shows the current peak height increase as a function of the concentration of iron ions in a 100 fM nickel ion solution. The maximum electrocatalytic amplification was achieved with a mixture of $\text{Ni}_{0.8}\text{Fe}_{0.2}$; however, the deviation in the measurement is about 50%, implying that the peak height measurements at 10, 15, and 20 fM iron ions are statistically similar. Above 40 fM iron ions in solution, no current spikes were observed in the amperometric $i-t$ response. It is surprising that the stochastic electrochemistry gives a similar result to that of bulk studies.

CONCLUSION

Electrocatalytic amplification has been used to observe small clusters of electrocatalytic metal oxide centers forming on a relatively inert UME. The detection is achieved by nucleating a small cluster from femtomolar solutions of the ionic precursor, such as solutions containing cobalt, nickel, or iridium ions. The potential of the electrode was applied such that water oxidation occurs minimally on the inert carbon fiber UME surface. The potential was also enough such that the metal oxide would electrodeposit and a catalytic response, such as a blip in the amperometric $i-t$ curve, could be observed. From an analysis of the frequency of the blip formation compared to the calculated frequency with which an ion should interact with the electrode, an estimated number of ions, capable of inducing water oxidation, can be calculated. Table 1 gives a summary of the results obtained in this study. This work is of fundamental interest in allowing a quantitative means of counting the number of atoms involved in the formation of a nascent catalytic cluster. The work is also of applied interest in the low limits of ion detection and is also interesting because the detection can be carried out under neutral pH conditions.

The technique was further used to investigate the catalysis between nickel and iron in an effort to investigate the nickel–

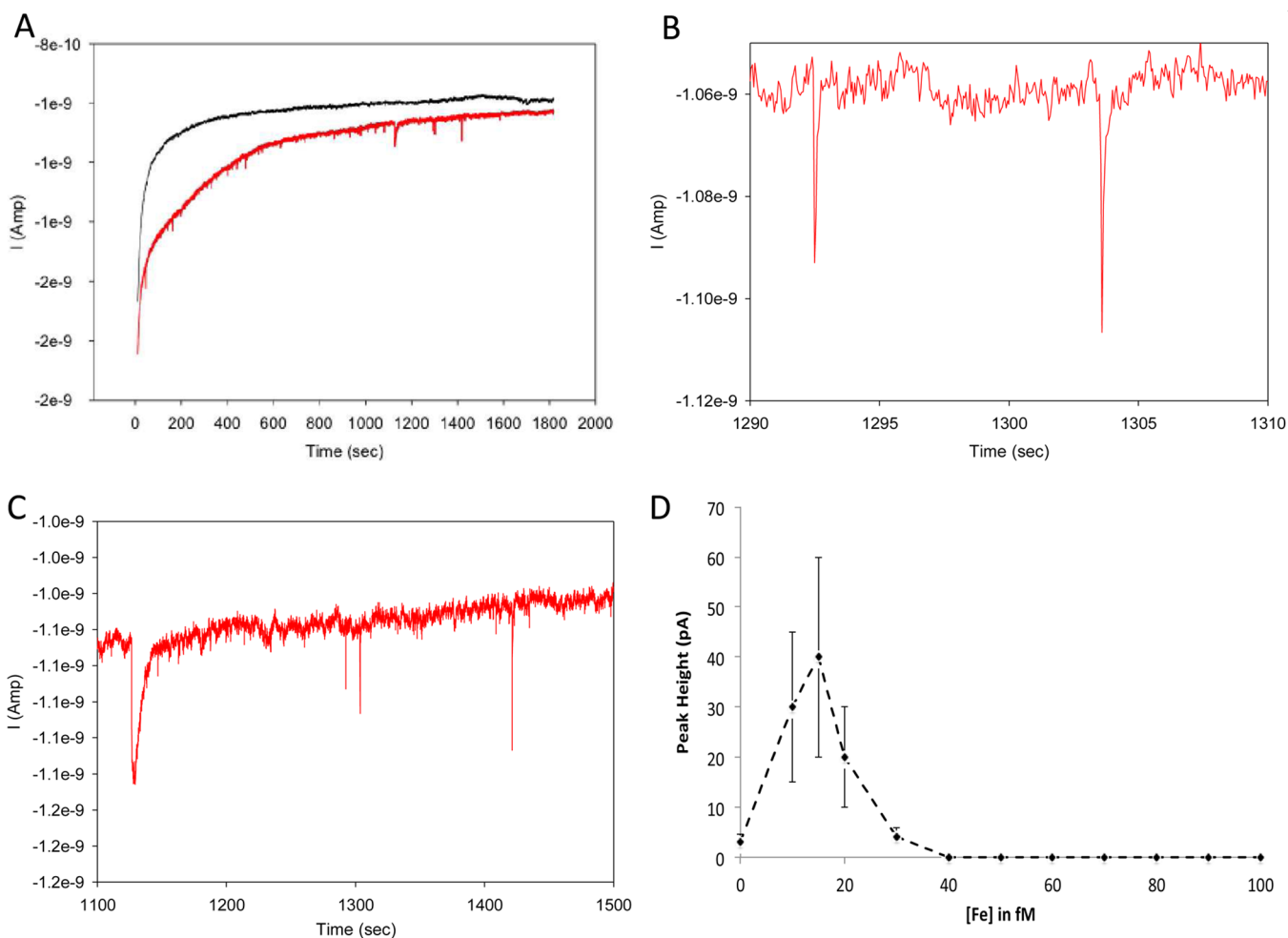


Figure 7. (A) Amperometric experiments of background oxidation (black trace) without nickel nitrate or ferrous chloride compared to 100 fM nickel nitrate and 15 fM ferrous chloride. (B and C) Enlargement of representative peaks. The sampling rate was 50 ms, and the applied potential was 1.4 V vs Ag/AgCl. (D) Blip height as a function of the amount of ferrous chloride added to solution. The concentration of nickel nitrate was held at 100 fM.

Table 1. Summary of the Minimum Number of Metal Atoms in an Electrocatalytic Cluster Calculated Using the Stochastic Electrochemical Technique

ion	no. ions (OER, freq)	no. ions (OER, t_{FE})	no. ions (HER, freq)
cobalt	10 ± 1	11 ± 2	–
iridium	13 ± 4	10 ± 3	6 ± 2
nickel	11 ± 3	–	–

iron amplification using the stochastic electrochemical technique. From these investigations, a ratio of 5:1 nickel to iron was found to give the largest responses in the amperometric $i-t$ response, which matches surprisingly well with previous reports with bulk materials. Given the results observing an increase in current peak height with nickel and iron ions, it should be possible to study how electrocatalysts are affected by mixing another metal.

AUTHOR INFORMATION

Corresponding Author

*ajbard@mail.utexas.edu

Notes

The authors declare no competing financial interest.

ACKNOWLEDGMENTS

This material is based upon work supported by the National Science Foundation Graduate Research Fellowship under Grant No. DGE-1110007, National Science Foundation Grant No. CHE-1405248, and the Welch Foundation (F-0021). J.D. also acknowledges Dr. Christophe Renault for helpful discussions.

REFERENCES

- (1) Dick, J. E.; Bard, A. J. *J. Am. Chem. Soc.* **2015**, *137*, 13752.
- (2) von Weber, A.; Baxter, E. T.; White, H. S.; Anderson, S. L. *J. Phys. Chem. C* **2015**, *119*, 11160.
- (3) von Weber, A.; Baxter, E. T.; Proch, S.; Kane, M. D.; Rosenfelder, M.; White, H. S.; Anderson, S. L. *Phys. Chem. Chem. Phys.* **2015**, *17*, 17601.
- (4) Luo, L.; White, H. S. *Langmuir* **2013**, *29*, 11169.
- (5) Ustarroz, J.; Hammons, J. A.; Altantzis, T.; Hubin, A.; Bals, S.; Terryn, H. *J. Am. Chem. Soc.* **2013**, *135*, 11550.
- (6) Fan, F.-R. F.; Demaille, C. The Preparation of Tips for Scanning Electrochemical Microscopy. In *Scanning Electrochemical Microscopy*, 2nd ed.; Mirkin, M. V., Bard, A. J., Eds.; Marcel Dekker: New York, 2001; pp 75–78.
- (7) Kanan, M. W.; Nocera, D. G. *Science* **2008**, *321*, 1072.
- (8) See, for example: Robertson, W. M. *J. Nucl. Mater.* **1969**, *30*, 36.

- (9) (a) Sousa, J. P.; Pons, S.; Fleischmann, M. *J. Chem. Soc., Faraday Trans.* **1994**, *90*, 1923–1929. (b) Abyaneh, M. Y.; Fleischmann, M.; Del Giudice, E.; Vitiello, G. *Electrochim. Acta* **2009**, *54*, 879–887.
- (10) Kwon, S. J.; Fan, F. – R. F.; Bard, A. J. *J. Am. Chem. Soc.* **2010**, *132*, 13165.
- (11) Smith, R. D. L.; Prevot, M. S.; Fagan, R. D.; Trudel, S.; Berlinguette, C. P. *J. Am. Chem. Soc.* **2013**, *135*, 11580.
- (12) Trotochaud, L.; Ranney, J. K.; Williams, K. N.; Boettcher, S. W. *J. Am. Chem. Soc.* **2012**, *134*, 17253.